

Lower San Pedro Groundwater Basin Profile



Basin Summary Statistics

Size¹: 1,624 square miles

Elevation²: Range: 1,735-8,561 ft; Median: 3,616 ft

Top 3 land cover types by area³: Shrub/Scrub (92%), Grassland Herbaceous (2.8%), Evergreen Forest (2.7%)

Major surface watershed(s)⁴: Lower San Pedro River, Middle Gila River

Groundwater subbasins¹: Camp Grant Wash, Mammoth

Groundwater-derived streamflow fraction⁵:

0.53 (High)



Mean Annual Hydrologic Cycle Components (1980-2020)
LOWER SAN PEDRO

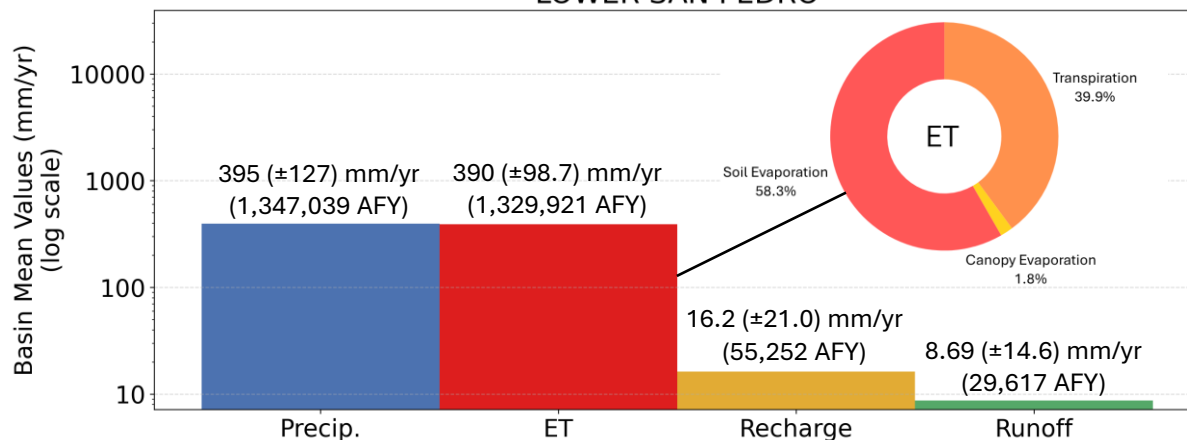


Figure 1 (above). Bar chart showing Noah-MP modeling results of the historical mean annual hydrologic cycle components (precipitation [P], evapotranspiration [ET], natural recharge, and runoff) in the basin from 1980-2020.⁶ ET is partitioned into soil evaporation, canopy evaporation, and transpiration. It is possible for ET to be greater than P when there are other sources such as groundwater, surface water, or water in storage.

Mean Monthly Hydrologic Cycle Components (1980-2020)
LOWER SAN PEDRO

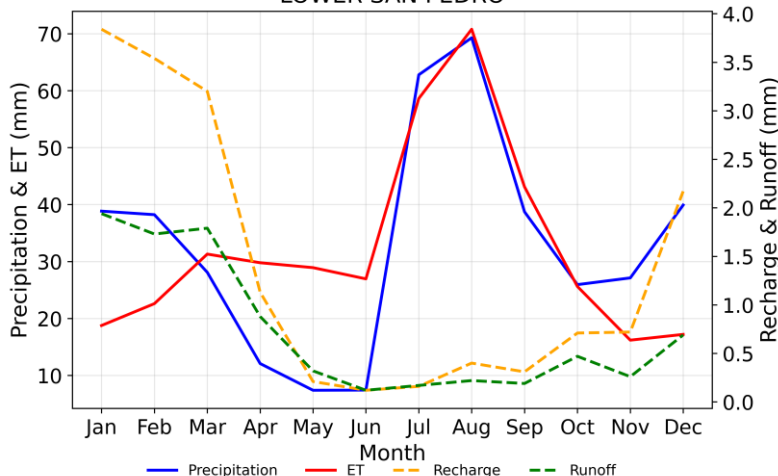


Figure 2. Graph showing monthly mean precipitation, ET, recharge, and runoff for the groundwater basin (1980-2020) from Noah-MP modeling results.⁶

On annual timescales, evapotranspiration (ET) is approximately equal to annual precipitation (P) across the basin, resulting in relatively low basin-wide annual averages for natural recharge (16.2 mm) and runoff (8.69 mm). P in the Lower San Pedro basin is affected by the North American Monsoon during the summer months. ET is approximately equal to P during these months due to enhanced water availability. ET exceeds P from March through mid-June. Soil evaporation makes up 58.3% of total ET in the basin, while transpiration comprises 39.9% and canopy evaporation accounts for the remainder (1.8%). Natural recharge and runoff are highest in January due to winter precipitation and relatively low atmospheric demand during the cooler months.

Lower San Pedro



Figure 3 (below). Gridded depiction of mean annual water fluxes across the groundwater basin from Noah-MP modeling (1980-2020): (a) precipitation, (b) evapotranspiration, (c) recharge, (d) runoff.⁶ Major cities/towns⁷ and Native American Reservation boundaries⁸ are shown (as applicable) to help orient the reader.

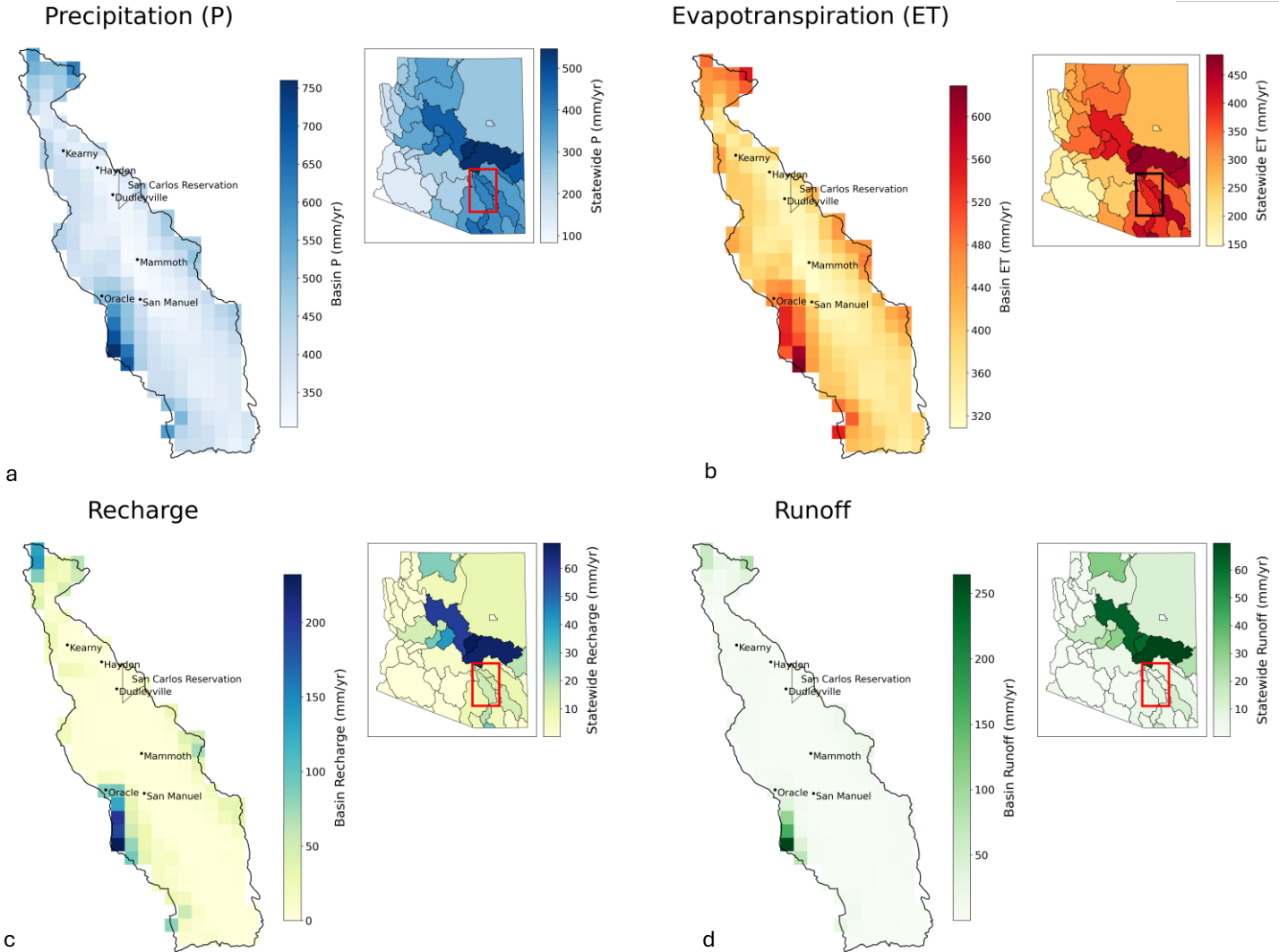
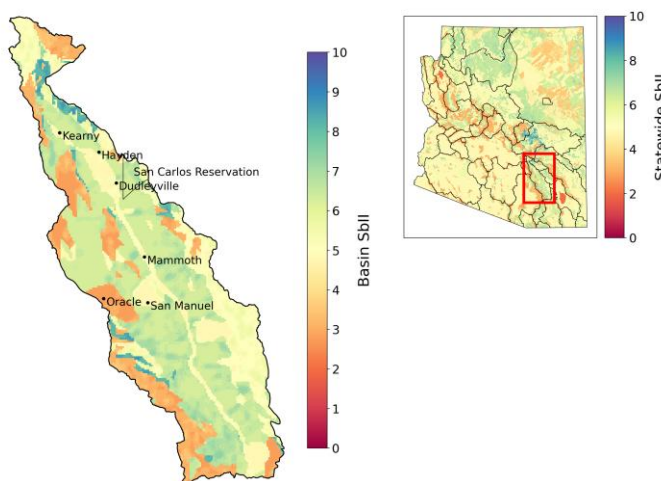


Figure 4 (below). Subsurface infiltration index (SbII) showing infiltration potential of the subsurface across the groundwater basin on a scale of 1-10 based on geologic features.⁹

Subsurface Infiltration Index (SbII)



Precipitation in the Lower San Pedro basin is highest in the Santa Catalina Mountains south of Oracle, which receive 700 mm/yr on average. The Santa Catalina Mountains also have the highest evapotranspiration (~550 mm/yr), natural recharge (~200 mm/yr), and runoff (~200 mm/yr) in the basin. Subsurface infiltration potential is moderately high across the basin, particularly in areas of moderately consolidated conglomerate that contain limestone to the east and west of the San Pedro River. High infiltration potential is found in the limestone-dominated formations of the Dripping Springs mountains north of Kearny and in the northern Santa Catalinas south of Oracle.

Lower San Pedro

Climate Change Projections: Changes in Temperature, Precipitation, ET, Recharge, and Runoff (2060-2099 vs. 1981-2020)

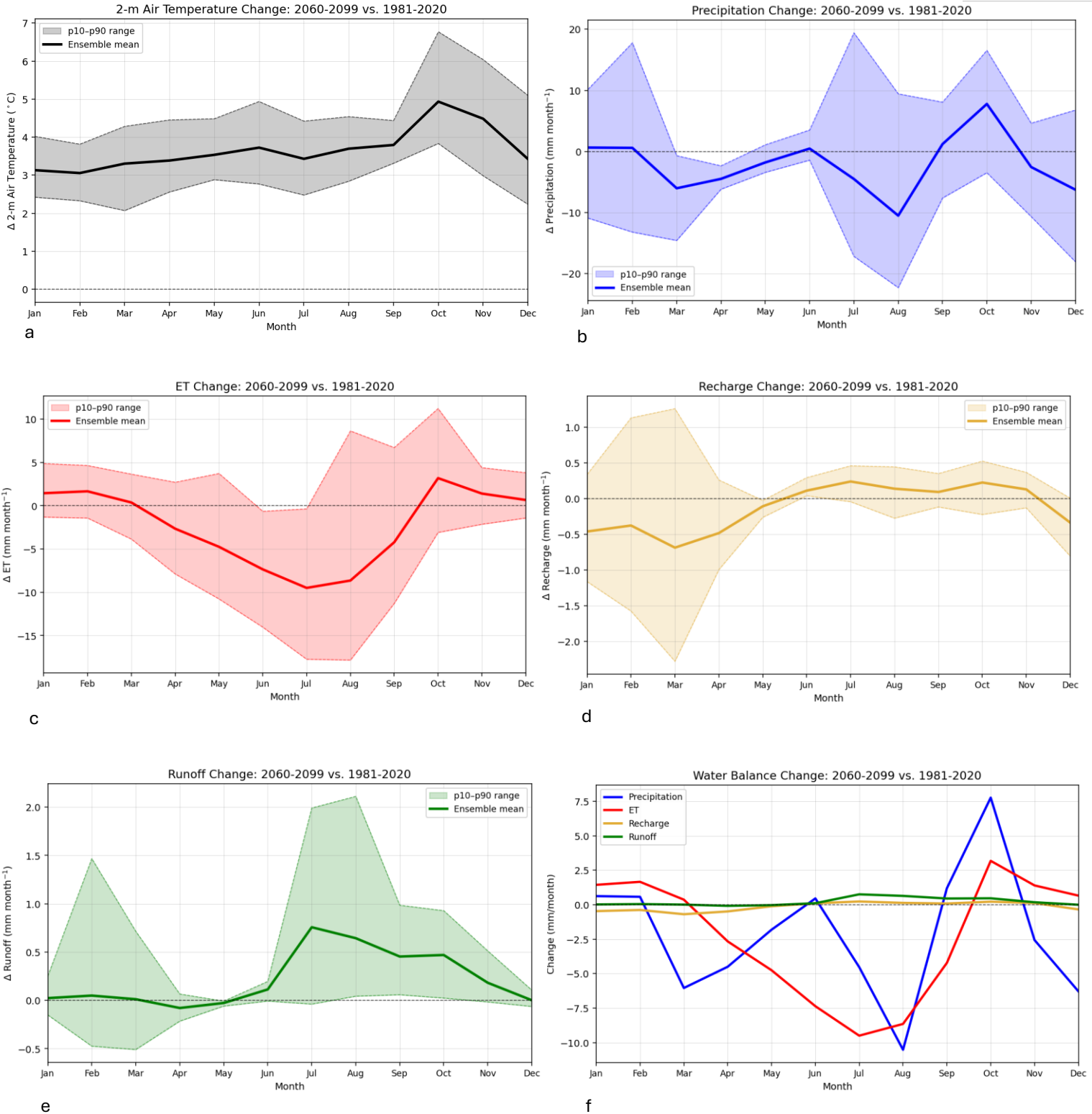


Figure 5. Plots (a)-(e) show projected changes in (a) temperature, (b) precipitation, (c) evapotranspiration (ET), (d) natural recharge, and (e) runoff statewide, comparing end of the 21st century to the historical record from 1981-2020 under the IPCC Scenario SSP3-7.0.¹⁰ Plot (f) shows the change in the water balance components (P, ET, recharge, and runoff) on a single graph for direct comparison. The analysis uses 14 dynamically downscaled global climate models (GCM) at 9-km resolution and the Noah-MP land surface model. The ensemble mean of the 14 GCMs is shown in bold for each component of the hydrologic cycle, with the 10-90th percentile shaded to show model projection uncertainty.

Lower San Pedro



Climate change projections across the Lower San Pedro basin show less precipitation throughout the majority of the year, with the exception of September and October, which show a 3-29% (1.2-7.8 mm/month) increase in precipitation. This increase in fall precipitation is consistent with a projected increase in extreme events associated with hurricane and tropical cyclone activity by the end of the century. The greatest declines in precipitation are projected for March-May (20-41%), July-August (7-15%), and November-December (11-15%). Declines in recharge ranging from 16-25% (-0.44 to -0.71 mm/month) are projected for highest recharge months from January to March. Despite showing less water loss from the system (i.e., a positive increase in Figure 8(d)), recharge projections are slightly negative (-0.11 to -0.21 mm/month) from June through August.* Runoff is projected to increase by 0.19 to 0.77 mm/month from July through November. Projected increases in temperature range from approximately 3.1 °C in February to 5.0 °C in October. Less water availability from precipitation in April-August leads to a projected 8-24% (-2.7 to -9.5 mm/month) decrease in evapotranspiration (ET) in those months, while higher temperatures and greater water availability lead to a projected 12% (3.2 mm) increase in ET in October compared to the baseline period.

*Projected negative recharge values are attributed to increased capillary rise from the aquifer through the vadose zone due to climate factors, resulting in water loss from the system. Because the Noah-MP model does not include groundwater pumping, this indicates that climate-driven factors play a significant role in groundwater storage decline in Arizona.

References

1. ADWR Groundwater Basin and Subbasin shapefiles. Retrieved from: <https://gisdata2016-11-18t150447874z-azwater.opendata.arcgis.com/>
2. USGS Digital Elevation Model data. Retrieved from: <https://apps.nationalmap.gov/downloader/>
3. Annual National Land Cover Database – Land Cover (2024). Retrieved from the Multi-Resolution Land Characteristics Consortium: <https://www.mrlc.gov/data>
4. USGS HUC8 Watersheds. Retrieved from: <https://hydro.nationalmap.gov/arcgis/rest/services/wbd/MapServer>
5. Mroczek, C., Springer, A. E., Gupta, N., Sankey, T., & Lucas, B. (2025). Regional base-flow index in arid landscapes using machine learning and instrumented records. *Journal of Hydrology: Regional Studies*, 62, 102778. <https://doi.org/10.1016/j.ejrh.2025.102778>
6. Gupta, A., Qiu, Y., Behrangi, A., & Niu, G. (2026). Noah-MP 40-Years Climatology for Water Balance over Ground Water Basins in Arizona, HydroShare, <http://www.hydroshare.org/resource/a3cc182071124849a463b6132213af23>. (Figures by Hinkley, M. & Mohsenzadeh Karimi, S.)
7. AZGeo City Points shapefile. Retrieved from AZGeo Data Hub: <https://azgeo-open-data-agic.hub.arcgis.com/datasets/azgeo::city-points/about>
8. Federal American Indian Reservation boundaries shapefile. Retrieved from: https://services2.arcgis.com/FiaPA4ga0iQKduv3/arcgis/rest/services/Federal_American_Indian_Reservations_v1/FeatureServer
9. Lima, R., Springer, A., Sankey, T. (2026). Arizona Subsurface Infiltration Index v.2, HydroShare, <https://doi.org/10.4211/hs.abcd8aa1a793463ab33677ce9d46db58>
10. Qiu, Y. (2026). Future Projection of Hydroclimate over Arizona Version 2, HydroShare, <https://doi.org/10.4211/hs.a5751f0af305483682501f79d9af0bd7>

